Journal of Materials Chemistry B

Materials for biology and medicine

Accepted Manuscript

Journal of
Materials Chemistry B

Materials for biology and medicine

rsc.li/materials-b

Volume 6
Number 3
21 January 2018
Pages 341-528

ISSN 2050-750X

ROYAL SOCIETY OF CHEMISTRY

PAPER
Wei Wei, Guanghui Ma et al
Macrophage responses to the physical burden of cell-sized particles

This is an Accepted Manuscript, which has been through the Royal Society of Chemistry peer review process and has been accepted for publication.

Accepted Manuscripts are published online shortly after acceptance, before technical editing, formatting and proof reading. Using this free service, authors can make their results available to the community, in citable form, before we publish the edited article. We will replace this Accepted Manuscript with the edited and formatted Advance Article as soon as it is available.

You can find more information about Accepted Manuscripts in the Information for Authors.

ROYAL SOCIETY OF CHEMISTRY

rsc.li/materials-b

1 **Injectable biocompatible hydrogels with tunable strength based on**

2 **crosslinked supramolecular polymer nanofibers**

3 Hans F. Ulrich,[a,b] Ceren C. Pihlamagi,[a,b] Tobias Klein,[a,b] Camille Bakkali-Hassani,[c] Sylvain

4 Catrouillet,[c] Johannes C. Brendel,[a,b,d,e],*

5 a Laboratory of Organic and Macromolecular Chemistry (IOMC), Friedrich Schiller University

6   Jena, Humboldtstr. 10, 07743 Jena, Germany

7 b Jena Center for Soft Matter (JCSM), Friedrich Schiller University Jena, Philosophenweg 7,

8   07743 Jena, Germany

9 c ICGM, Univ. Montpellier, CNRS, ENSCM, 34095 Montpellier, France

10 d Macromolecular Chemistry I, University of Bayreuth, Universitätsstr. 30, 95447 Bayreuth,

11   Germany

12 e Institute of Macromolecular Research (BIMF) and Bavarian Polymer Institute (BPI),

13   University of Bayreuth, Universitätsstr. 30, 95447 Bayreuth, Germany

14 *corresponding author: johannes.brendel@uni-jena.de

17 Abstract

18 Hydrogels based on supramolecular assemblies offer attractive features for biomedical applications

19 including injectability or versatile combinations of various building blocks. We here investigate a

20 system combining benzenetrispeptides (BTP), which forms supramolecular fibers, with the

21 polymer polyethylene oxide (PEO) forming a dense hydrophilic shell around the fibers. Hydrogels

22 are created through addition of a bifunctional crosslinker (CL). Rheological studies revealed that

23 shorter hydrophobic n-hexyl spacers (BTP-C$_6$) lead to stronger hydrogels than the BTP-C$_{12}$

24 comprising n-dodecyl chains. All hydrogels recover rapidly (< 5 s) after deformation in step-strain-

1

25 measurements. We varied the crosslinker content between 0.1, 1 and 10 mol% and the overall

26 concentration of the gelator. While the shear storage modulus of all BTP-C$_{12}$ hydrogels remains

27 below 1 kPa independent of the variations, the shear storage modulus BTP-C$_6$ hydrogels can be

28 tuned from around 0.2 kPa up to almost 8 kPa. Shear rate dependent viscosity measurements

29 further revealed similar shear thinning behavior of all hydrogels, and calculation of extrusion

30 parameters confirms that the hydrogels can easily be injected even through thin cannulas.

31 Accordingly, we injected a fluorescein containing BTP-C$_6$ sample into chicken breast

32 demonstrating the potential for application as injectable drug depot. Furthermore, BTP-C$_6$

33 hydrogels prevent adherence of L929 mouse fibroblasts but preserve their relative metabolic

34 activity (>87%) during incubation on the gel when compared to cells growing on adherent surfaces.

35 Our investigations overall reveal that particularly the BTP-C$_6$ system has attractive features for

36 applications in tissue engineering or as injectable and biocompatible drug depot.

Introduction

37

38 A plethora of examples regarding self-assembly processes of biomacromolecules in nature (e.g.

39 nucleic acids, proteins, and polysaccharides) has inspired the research on supramolecular based

40 hydrogels and their biomedical applications such as tissue regeneration, drug delivery and artificial

41 cell scaffold.[1-3] Dissimilar to conventional synthetic hydrogels, which are made of three-

42 dimensional networks of polymer chains linked by permanent covalent bonds, supramolecular

43 hydrogels form through self-assembly of small organic molecules (hydrogelators) by noncovalent

44 interactions.[4-9] These intermolecular forces often result in a dynamic system at room temperature,

45 where a liquification (viscous flow) of the supramolecular hydrogels can occurs given a sufficient

46 shear force (shear thinning) and the system recovers once the applied force is removed (self-

47 healing).[3] The peculiar viscoelastic properties and self-healing ability of supramolecular hydrogels

48 make them promising candidates for applications, such as injectability for tissue engineering or

49 drug delivery.[1, 2, 10-14]

50 Ureido-pyrimidinone, peptides, benzenetrisamides, and benzenetrisurea are common examples of

51 supramolecular motifs of hydrogels displaying shear thinning behavior.[15-22] These systems mainly

52 rely on H-bond interactions and on hydrophilic polymers, mostly polyethylene oxide (PEO), which

53   are functionalized on their end groups with the corresponding supramolecular motifs. There are

54   different ways these motifs can be utilized. One approach uses the interactions of the end groups

55   in star or branched polymers to form a large crosslinked network in which the end groups form

56   junctions sides that act as linkage between the PEO chains.[23-26] A different approach utilizes

57   hydrophobic supramolecular motifs such as ureidopyrimidinone, benzenetrisamides and

58   benzenetrisureas (BTU) decorated with hydrophilic groups to obtain amphiphilic molecules, which

59   are able to form fibers through self-assembly.[16, 22, 27, 28] An advantage of fiber formation, is that

60   through overlapping of the fibers or defects in the structure junction sides are formed, which lead

61   to gel formation.[29] Even though some of these systems already form hydrogels without a special

62   crosslinker, the gels become stronger when a homotelechelic polymer with the motif on both end

63   groups is utilized as a crosslinker. Here the crosslinker is integrated during the assembly step to

64   ensure an even distribution throughout the fiber. In respect of biological applications, fast recovery

65   kinetics and the optimum shear force are crucial parameters when designing supramolecular

66   hydrogels.[30, 31] For instance, fast recovery rates were observed in hydrogels based on peptides.[19,

67   32, 33]

68   Previously, our group demonstrated that the BTU motif is able to form hydrogels with a strong

69   shear thinning character enabling 3D printing.[28] Although these results are promising, BTUs allow

70   almost no modification of their hydrophobic interactions by varying the spacers nor any changes

71   of the hydrogen bonding units without disturbing the assembly process.[34] These aspects limit the

72   adaptability of the hydrogels in terms of mechanical or rheological properties, which are crucial

73   for cell and tissue interactions. Therefore, we explored benzenetrispeptide (BTP) based

74   supramolecular motifs, which form self-assembled fibers when conjugated with PEO chains that

75   can be varied in their length by adjusting the kinetics of the assembly process.[35, 36] The strong

76   interaction of the BTP allows more variations of the hydrophobic groups as for the benzenetrisurea

77   motif and, for example, n-hexyl (C_6) or n-dodecyl (C_{12}) chains can both be employed as

78   hydrophobic spacers.[35, 37] Moreover, recent investigations revealed that the BTP system shows a

79   stronger tendency to form supramolecular fibers compared to the BTU system, even when more

80   complex hydrophilic polymers are utilised.[38] The robustness during the fiber assembly and

81   versatility make BTP system a promising candidate for future applications. We conducted multiple

82   rheological measurements on both BTP-C_6 and BTP-C_{12} based hydrogels varying conditions such

3

83 as the crosslinker content from 0.1-10 mol% and overall concentration for 25 and 50 mg mL^{-1}.

84 Furthermore, we examined rheological behavior of the hydrogels at temperatures between 0-80 °C.

85 To reveal the biomedical applicability for future studies, the injectability and recovery of the gel in

86 a biological environment were qualitatively assessed by injection of a fluorescein containing BTP-

87 C_6 hydrogels into muscle tissue (chicken breast sample). In addition, the viability of L929 mouse

88 fibroblast cells growing on the BTP-C_6 hydrogels was determined.

89 **Results and discussion**

n	Monomer	Crosslinker
2	BTP-C_6	CL_6
5	BTP-C_{12}	CL_{12}
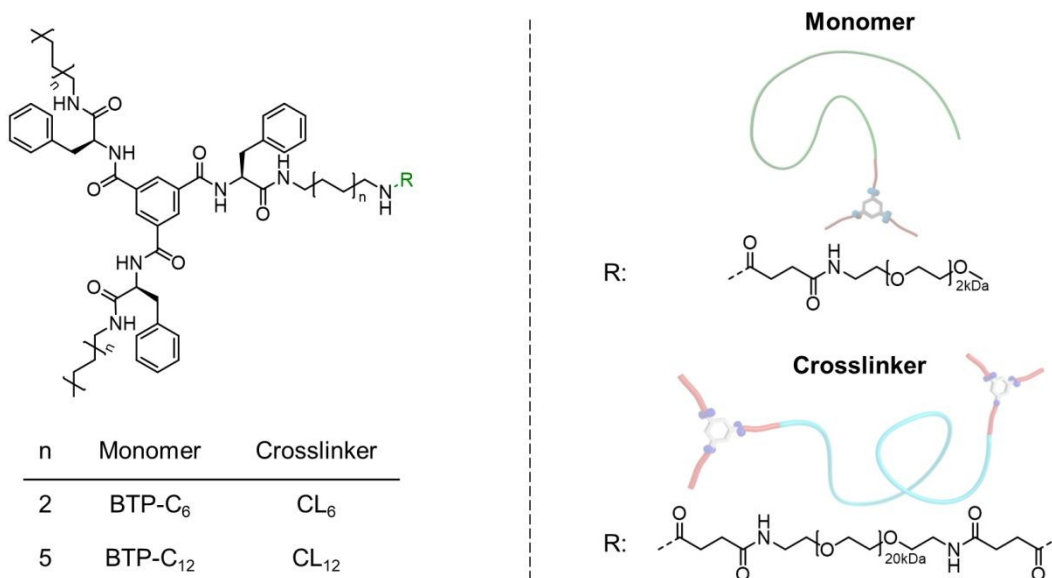
90

91 **Fig. 1.** Overview of the chemical structures of the prepared benzenetrispeptide based monomers
92 and crosslinkers.

93 The synthesis of BTP-monomer and crosslinker (CL) units (**Fig. 1**) was performed according to

94 the procedures established by Gruschwitz and Klein.[28, 35] For the confirmation of the successful

95 PEO attachment, ^{1}H-NMR (see SI) and size exclusion chromatography (SEC) measurements

96 (**Fig. 2**) were performed. The SEC measurements of the monomer units showed monodisperse

97 distribution in their elugrams (**Fig. 2a**). Interestingly, a shoulder towards higher molar masses was

98 observed for CL_{12} (**Fig. 2b**) although no evidence of side reactions was observed in the NMR

99 spectra. Therefore, we assume that this occurrence is a result of dimerization of CL_{12} in the SEC

100 solvent (DMAc + 0.21wt% LiCl), which indicates poor solubility and strong interaction.

101
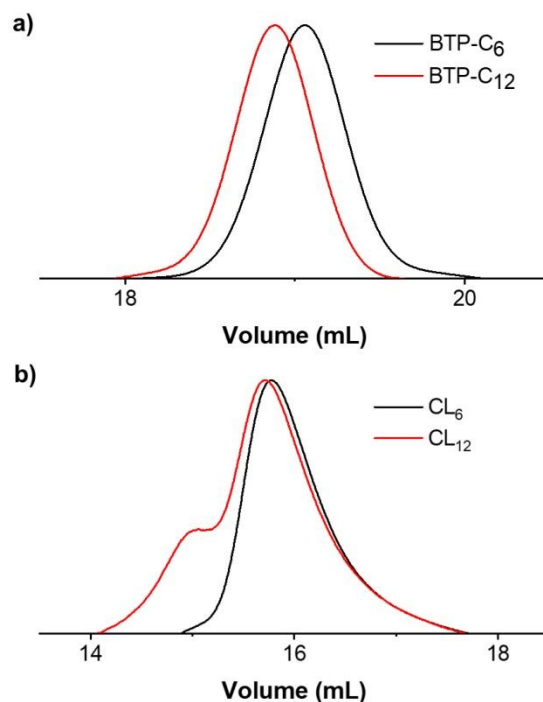
Fig. 2. Overview of SEC measurements, showing elugrams of the BTP-monomer (**a**) and BTP-crosslinker units (**b**). Measured using DMAc (+ 0.21*wt*% LiCl) as eluent and a flow rate of 1 mL min^{-1}.

Multiple parameters were considered for the rheological investigation to assess the potential of the BTP based hydrogels for biomedical applications.[39] Based on previous experience, the conditions for the first experiment were set to a sample concentration of 25 mg mL^{-1} and a crosslinker concentration of 1 mol%.[28] Maintaining comparable weight contents of the supramolecular building blocks, the difference of molar mass between BTP-C$_6$ and BTP-C$_{12}$ causes slight discrepancies in their final molar concentrations (approximately 0.7 µmol mL^{-1}). For the general hydrogel preparation procedure, we mixed the BTP-monomer and crosslinker and dissolved them in THF. To ensure that the system was fully dissolved, the solutions were heated to ~40°C. In case of the BTP-C$_6$ system, a small amount of water (<50 µL) was necessary for complete dissolution, as the system gelled in pure organic solvent (THF) after cooling down. A gradual solvent switch from THF to water was then performed by slowly adding water (syringe pump at 1 mL h^{-1}) to the organic mixture reaching a content of 67% water, before the organic solvent was finally removed by evaporation. This procedure results for both samples BTP-C$_6$ and BTP-C$_{12}$ in free standing hydrogels (**Fig. 3a**). Additionally, we also assessed the capability of the systems to form hydrogels

Journal of Materials Chemistry B Accepted Manuscript

119 in the absence of crosslinker at the given concentrations, but we did not observe any hydrogel

120 formation for both samples (**Fig. 3b**).

121 As the first step of rheological studies, we examined the linear viscoelastic domain of our samples

122 *via* a stress sweep measurement in order to determine how much stress we can apply to our sample,

123 without breaking the gel structure, yet (**Fig. 3c & d** see SI section 2.2 stress sweep measurements

124 of all samples). Shear storage modulus (G') and loss modulus (G'') are stable when subjected to a

125 shear stress from 0.4 to 10 Pa for both samples. Therefore, we choose a shear stress of 1 Pa for

126 further measurements of both samples.

127
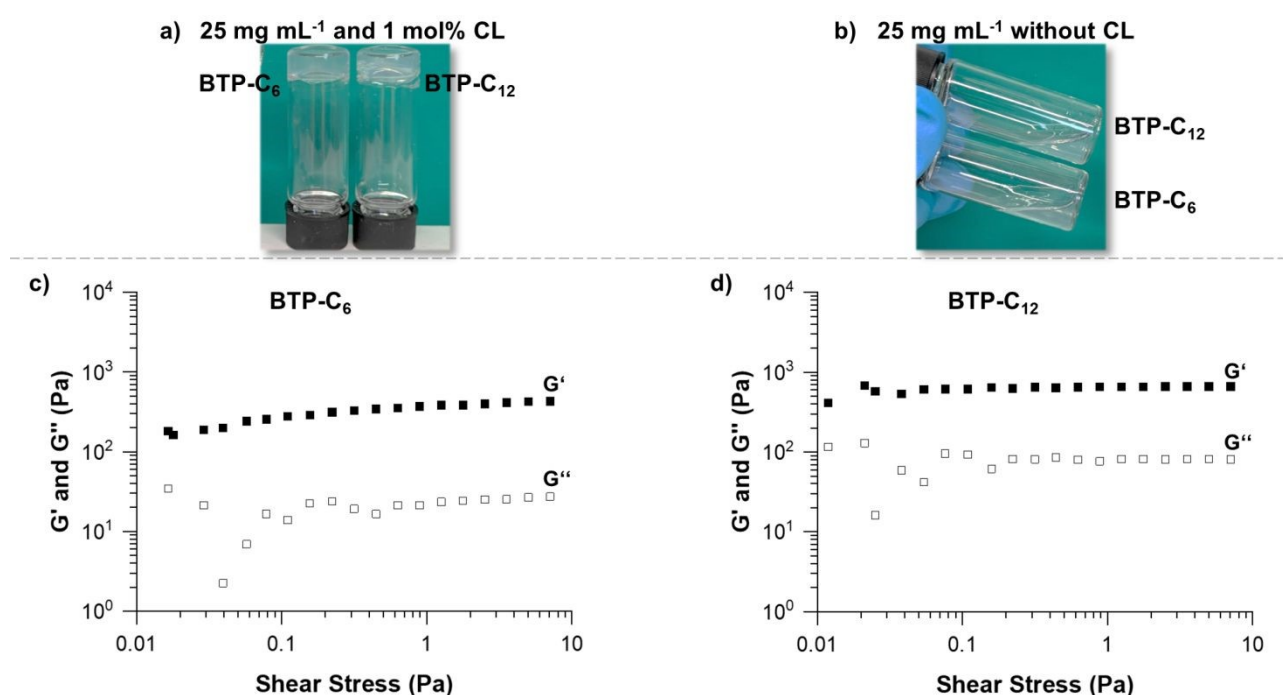
Fig. 3. Images of the hydrogels (c = 25 mg mL^{-1}) with 1 mol% crosslinker (a) and without
crosslinker (b). Stress sweep of the BTP-C$_6$ (c) and BTP-C$_{12}$ hydrogels (d) at 20 °C to determine
the stress strength usable for further tests.

131 As the first major investigation, we conducted step-strain measurements. During this measurement

132 the sample is multiple times deformed applying a large strain (200 % deformation) and allowed to

133 recover, which yields information on the self-healing properties of the hydrogels, i.e. if the sample

134 recovers and how long it needs to regain its initial strength.[40] Surprisingly, the BTP-C$_6$ system with

135 1 mol% crosslinking formed a significantly stronger hydrogel with an average G' value of ~1.1

136   kPa (**Fig. 4a**, red squares), whereas the BTP-C_{12} system resulted in a lower G' value of ~500 Pa

137   (**Fig. 4b**, red squares) at similar concentrations. We initially anticipated the formation of stronger

138   hydrogels by BTP-C_{12} motifs in comparison to BTP-C_6 counterparts due to the longer alkyl chains

139   present in BTP-C_{12}. A longer aliphatic chain is expected to enhance the hydrophobic interaction,

140   and thus should induce a higher stability of the self-assembled fibers in the gel. The lower modulus

141   of the BTP-C_{12} hydrogel might be related to a preaggregation of CL_{12} in THF (already observed in

142   SEC experiments) and, subsequently, an insufficient incorporation into the fiber network or

143   clustering of the crosslinker during the assembly process (**Fig. 4c & d**).
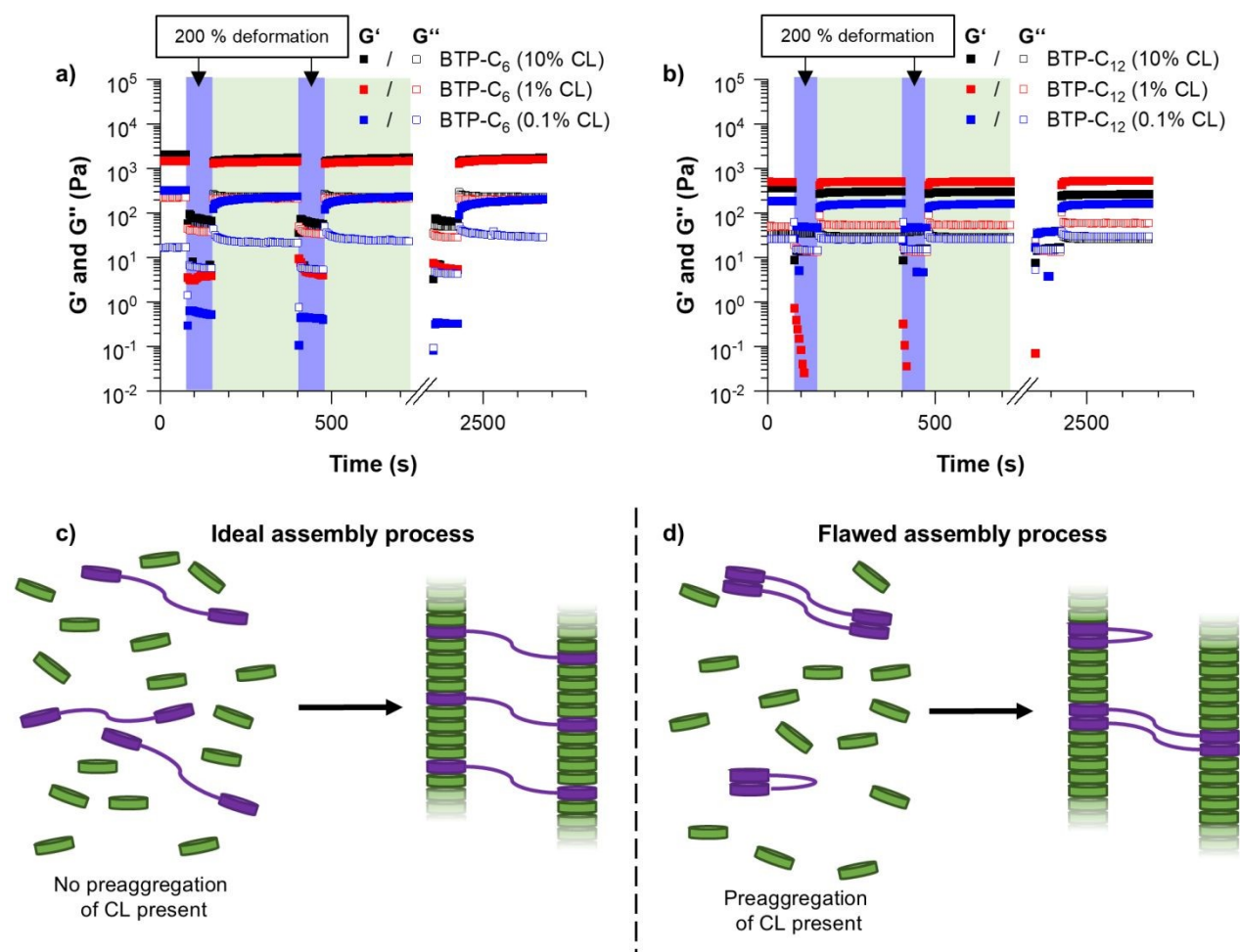
144

145   **Fig. 4.** Step-strain measurements of BTP-C_6 (a) and BTP-C_{12} (b) hydrogels with varying
146   crosslinker concentrations of 0.1, 1 and 10 mol% at 20 °C. Schematic representation of assembly
147   formation without (c) and with (d) and preaggregation of the crosslinker.

148 Concerning the capability of both systems to reform a gel after shear deformation, the rheological

149 measurements revealed a rapid recovery within less than 5 seconds over several cycles

150 strain/recovery. Only in the case of BTP-C_6 a slight decrease of shear storage modulus was

151 observed after the first strain step, followed by a gradual increase over time during each recovery

152 step. To further verify the robustness of the systems, we performed frequency sweep experiments

153 before and after the step strain measurement, which show only little variation indicating a full

154 recovery of the systems (Fig. S3 & S7).

155 Following these initial investigations on the BTP-C_6 and BTP-C_{12} systems, we explored the

156 influence of various crosslinker concentrations (0.1, 1, and 10 mol% CL) to evaluate its impact on

157 the mechanical properties of the hydrogels. We examined both systems analogously to the previous

158 measurements. For the BTP-C_6 system, we observed a slight increase in the G' value of the

159 hydrogels from ~1.4 kPa to ~1.7 kPa with 10 mol% CL and a significant decrease in the G' value

160 to ~0.2 kPa for 0.1 mol% CL (**Fig. 4a,** for individual measurements Fig. S3- S5). These findings

161 were in the line with our expectation because a higher crosslinking density leads to a higher stability

162 of the hydrogel and thus a higher G' value.[41] The 10 mol% CL sample featured a similar decreased

163 strength after the first step and gradual improvement as the initially tested sample with 1 mol% CL.

164 In case of the 0.1 mol% CL sample, however, the recovery occurs more slowly and requires several

165 minutes to reach a plateau level again. Surprisingly, the BTP-C_{12} system revealed lower G' values

166 at higher (10 mol%,) CL content compared to the initial tested sample with 1 mol% CL (~0.5 kPa)

167 (**Fig. 4b,** for individual measurements Fig. S7- S9). This weakening of the gel with increasing CL

168 content supports our hypothesis, that the limited solubility of CL_{12} causes a decrease in strength

169 compared to the CL_6 system. Furthermore, decreasing the CL content to 0.1 mol% has a less

170 pronounced effect on gel strength (~0.15 kPa compared to ~0.3 kPa for 1 mol% CL) than observed

171 for the BTP-C_6 system. All gels based on BTP-C_{12} recovered quickly (gel formation < 5 s) and a

172 plateau is rapidly reached for 10 mol% and 1 mol% CL, while the low CL content of 0.1 mol%

173 again causes a slight delay.

174

175
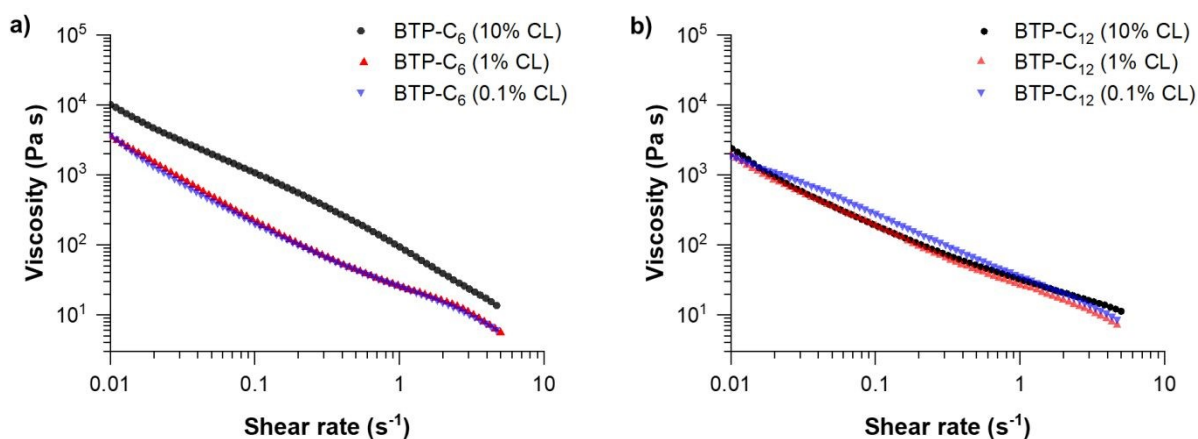
Fig. 5. Viscosity measurements of BTP-C_6 (a) and BTP-C_{12} (b) hydrogels with varying crosslinker concentrations of 0.1, 1 and 10 mol% at 20 °C. For individual measurements with measuring points below 0.01 s^{-1} see Fig. S3-5 & S7-8.

We further conducted shear viscosity measurements to reveal the effect of the crosslinker concentration on yield stress and the shear dependent viscosity of BTP-C_6 and BTP-C_{12} systems (**Fig. 5**). These are critical parameters to determine the pressure required to induce flow of the gel and evaluate the injectability of the hydrogels. Therefore, we applied a continuously increasing shear rate $\dot{\gamma}$ to determine its influence on the viscosity. We evaluated the results by using a power law fit on the linear regions at higher shear rates according to

$$\textbf{Eq. 1} \qquad \boldsymbol{\eta = K\dot{\gamma}^{n-1}}$$

These fits allowed us to determine the shear-thinning parameter *n* and consistency index *K* for the tested samples (**Table 1**).[30, 42] Additionally, we investigated the reversibility of the BTP-C_{12} system (1 mol% CL) to assess whether the viscosity of our system remains consistent based on multiple measurements. Therefore, we performed three consecutive runs by alternating between increasing and decreasing the shear rate (Fig. S11). The results revealed minimal variations demonstrating the robustness of our measurement setup and the stability of our system.

192

193

194 **Table 1.** Yield stress and fitted shear-thinning parameter n, consistency index K of BTP-C_6 and
195 BTP-C_{12} hydrogels with different crosslinker concentrations. The yield stress was determined at
196 the highest point before liquification set in during the viscosity measurements. The values for n
197 and K were obtained by applying a power law fit (**Eq. 1**) to the linear regression regions of**Fig. 4**
198 **5a & 5b**.

Sample	Crosslinker content (mol%)	Yield stress (Pa)	n	K (Pa s^{-1})
	10	70.1	0.08 ± 0.01*	122.95 ± 1.86*
BTP-C_6	1	32.3	0.14 ± 0.01	25.12 ± 0.36
	0.1	28.22	0.14 ± 0.02	24.31 ± 0.70
	10	17.7	0.30 ± 0.02	33.35 ± 0.93
BTP-C_{12}	1	13.6	0.16 ± 0.02	25.48 ± 1.31
	0.1	10.3	0.10 ± 0.01	33.89 ± 0.33

199 *Due to the abnormal curve progression of the measurement, the fit was applied to lower sheer
200 rates between 0.02-0.3 s^{-1}.

201 For all samples, the calculated values for n are well below 1 which corresponds to a strong shear-
202 thinning fluid, as the viscosity decreases significantly with increase of the shear-rate. Comparing
203 the previously reported benzenetrisurea systems, the obtained values for n and K are in a similar
204 range ($n = 0.15$; $K = 22.97$) proving that this shear-thinning behavior is characteristic for these
205 types of hydrogelators.[28] In addition, both systems indicate significantly lower values compared to
206 state-of-the-art printable polymer hydrogels based on poloxamer polymers ($n = 0.13$; $K = 406$) or
207 alginates ($n = 0.31$; $K = 254$).[42] Among the obtained results (**Table 1**), lower shear rates between
208 0.02-0.3 s^{-1} were applied for BTP-C_6 with 10 mol% CL due to the distinct behavior of the material
209 with higher shear rates (**Fig. 5a**). At higher shear rates >0.1 s^{-1} the value of n is negative ($n = -0.15$
210 ± 0.01; $K = 91.36 \pm 0.59$), which is related to a rather steep slope of the viscosity change with
211 increasing shear rate. Although such values are unusual, negative n values were also observed in
212 other studies.[43, 44] A plausible explanation for this anomaly could be that the sample becomes more
213 fragile with increasing crosslinker content.

214 The obtained values of n and K can also be used to calculate the pressure and force needed to
215 extrude the hydrogel through a cannula, and so their injectability can be determined.[30] Using the
216 predetermined parameters, we calculated the force needed to extrude the hydrogel through a

10

217   cannula of certain gauges (see SI Chapter 3 and Table S2). For a gauge 21 cannula, with a length

218   of 50 mm, commonly used for intramuscular injections, and a 1 mL syringe, BTP-C_6 and BTP-C_{12}

219   hydrogels with 1 mol% CL would require 0.62 N and 0.76 N force, respectively, to be extruded

220   with a flowrate of 0.1 mL s^{-1}. A gauge 23 cannula, with a length of 12 mm, commonly used for

221   subcutaneous injection, on the other hand, would require a force of 0.33 N for BTP-C_6 and 0.42 N

222   for BTP-C_{12} under the same conditions.[45] In all cases the required forces are considerably lower

223   than the maximum forces considered for manual (40 N) or automatic injection (20 N) of 1 mL with

224   an injection rate of 0.1 mL s^{-1}.[46] It is noteworthy, that the injection into tissue also affects the

225   necessary force due to the tissues counterpressure, which leads to an increase in the force needed

226   for e.g. subcutaneous injection.[47] As a proof of concept for the injectability of the hydrogels into

227   muscular tissue, we used a piece of chicken breast and injected the BTP-C_6 gel with a syringe. This

228   test should not only allow practical evaluation of the required injection forces, but also if the

229   hydrogel recovers in such an environment (**Fig. 6**). We used a 1 mol% crosslinked BTP-C_6 hydrogel

230   soaked with 1 mg mL^{-1} fluorescein, which resembled an easy traceable model compound here. For

231   the injection a gauge 23 cannula with a length of 80 mm and a 2 mL syringe were used, which still

232   allowed an easy and effortless manual injection of the hydrogel. The observed resistance was

233   similar to extrusion of a viscous oil. After sample injection (~0.2 mL) we lightly "massaged" the

234   sample to simulate muscle movement and cut the tissue to reveal the injection site. The hydrogel

235   appears to be distributed between different muscular cords but remains localized in the injection

236   area. It is noteworthy to mention, that neither the massaging nor the cutting of the chicken breast

237   had a strong impact on the distribution highlighting the stability of the gel even when injected into

238   tissue.

239
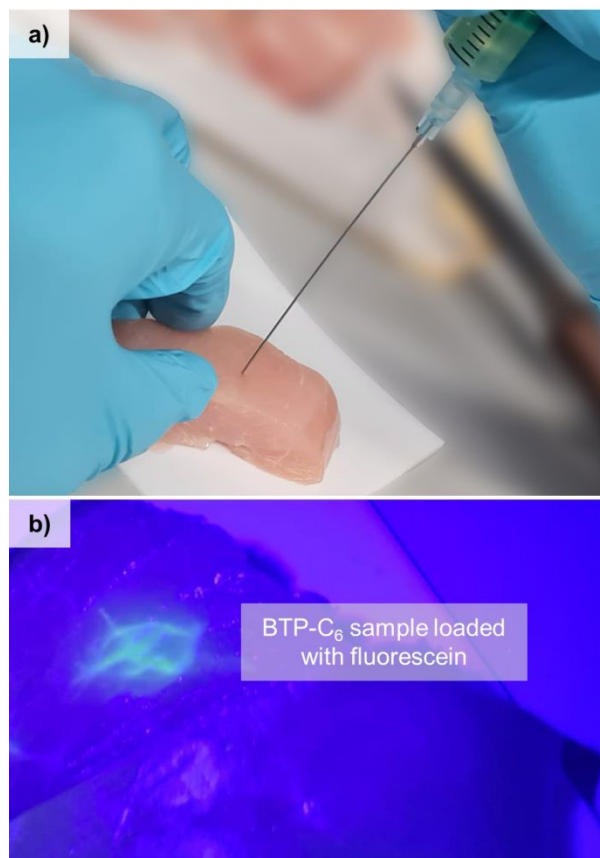
Fig. 6. Injection of a BTP-C$_6$ 1 mol% CL sample (using a G27 cannula), loaded with 1 mg mL^{-1} fluorescein as modal system, into chickenbreast (a). and a crosssection of the injectionside under UV light (b).

In order to explore the further potential of the materials, we analyzed the influence of the overall concentration of the gelator on G' value. A higher concentration should lead to a higher density of fibers in the hydrogel, which in return should lead to increased entanglements and, thus, a strengthening of the gel.[48, 49] We therefore kept the CL content at 1 mol% and increased the overall weight concentration of the BTP-system in the hydrogel from 2.5 wt% to 5 wt%, which in previous investigations on the benzenetrisurea system resulted in a noticeable (~three-fold) increase of the gel strength.[28] The G' values of the BTP-C$_6$ system increased to ~8 kPa (**Fig. 7a**), which is almost a six-fold increase compared to the sample with 2.5 wt%. To our surprise, the increase in concentration caused only an increase in strength from 0.3 kPa to ~0.8 kPa for the BTP-C$_{12}$ system (**Fig. 7b**). We assume that in the latter case the higher concentration of building block and

253   crosslinker further impedes the homogeneous distribution of the crosslinker over all fibers, which

254   is in accordance with the observations made for an increased crosslinker content.
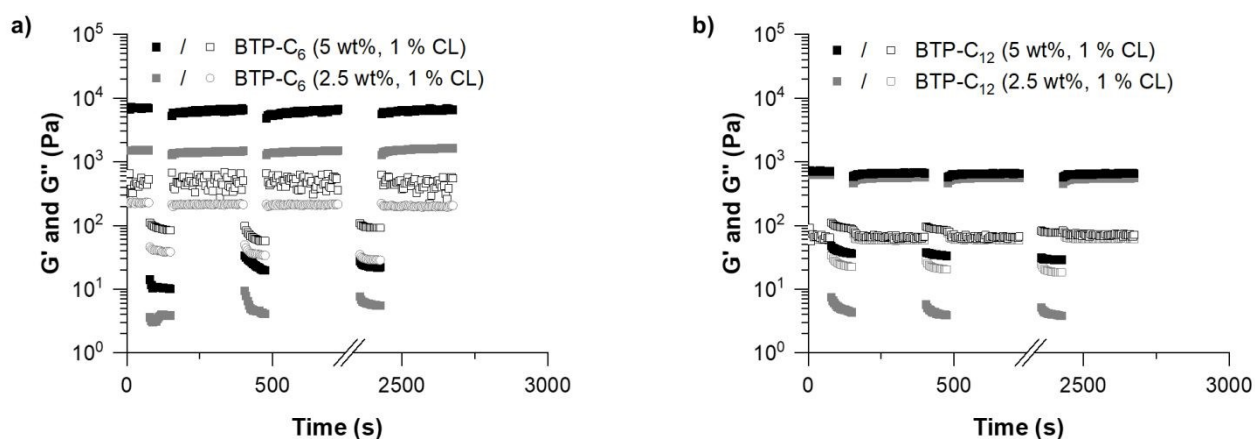
255

256   **Fig. 7.** Comparison between the hydrogels with concentrations of 2.5 wt% (grey) and 5 wt% (black)
257   based on BTP-C_6 (a) and BTP-C_{12} (b) with 1 mol% crosslinker at 20 °C.

258   Following these tests, we further evaluated the impact of increasing temperatures on the hydrogels.

259   Supramolecular interactions typically get weaker at elevated temperatures.[50] In our tests, the BTP-

260   C_{12} samples demonstrated such a weakening as the gel strength decreased from ~0.4 kPa at 0 °C to

261   ~0.15 kPa at 80 °C (**Fig. 8**), which is reversible through cooling of the sample (see Fig. S12).

262   Contrary, the BTP-C_6 sample showed an increase in G' from ~1.4 kPa to ~2.7 kPa (**Fig. 8**), which

263   indicates an unexpected thermal stiffening behavior. Such effects are less common for

264   supramolecular assemblies and could be due to changes in the aggregation structure.[51, 52] For

265   example Chakravarthy *et al.* proposed the formation of a double network at elevated temperatures

266   for their system, which leads to thermostiffening behavior at 37 °C.[53] Further investigations into

267   the cause of this phenomenon are currently ongoing, but considering a limited reversibility of the

268   BTP-C_6 sample we refrained from further temperature dependent measurements.

269
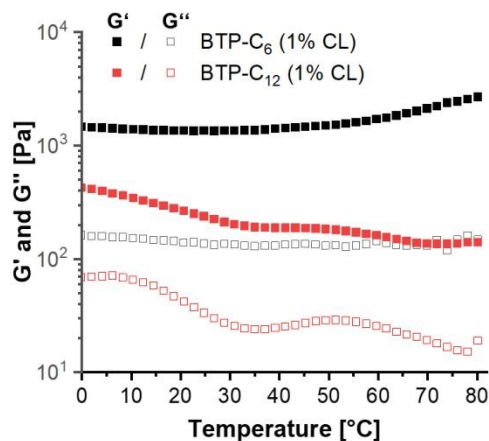
Fig. 8. Temperature sweep measurements from 0 to 80°C of BTP-C$_6$ (black) and BTP-C$_{12}$ (red) samples containing 25 mg mL^{-1} monomer and 1 wt% crosslinker.

As the BTP-C$_{12}$ system was more reliable with temperature changes we further investigated the temperature dependent stress relaxation behavior of the corresponding hydrogels. Isothermal stress relaxation experiments were performed at 5°C, 40°C, 60°C and 80°C (**Fig. 9a**) on the BTP-C$_{12}$ system (containing 1 mol% of crosslinker). The obtained data were normalized after 20 seconds of applied strain (1%, within the linear viscoelastic domain), this delay was necessary to reach a stable strain and reduce signal noise observed at the early stage of the experiments. As expected, the stress decay was faster at high temperatures which we attribute to a faster exchange of supramolecular crosslinker or network reorganization. By analogy with covalent adaptable networks, i.e. thermosets containing covalent exchangeable bonds, stress relaxation behavior of BTP-C$_{12}$ system can be describe by a multimode Maxwell Model (or KWW model) in which multiple relaxation mode coexist instead of a simple mode.[54, 55] The obtained data from **Fig. 9a** was accurately fitted (0.993 <R^2<0.998) using the following equation:

$$\text{Eq. 2} \qquad G(t) = G_o \exp\left(-\frac{t}{\tau}\right)^{\beta}$$

Fitting the stress relaxation behavior with this stretched exponential function reveals that at 5°C a broad relaxation time distribution is present ($\beta_{(5°C)}$ = 0.32), which gets "narrower" at higher temperatures ($\beta_{(80°C)}$ = 0.81). The activation energy E$_A$ = 37.8kJ.mol^{-1} (**Fig. 9b**) was extracted from the Arrhenius plot of ln(τ) vs 1/T where τ is the average relaxation time determined from stretched exponential fitting. These results indicate that the system becomes more dynamic with increasing

14

290 temperature, which is in accordance with behavior of other supramolecular systems. Further studies

291 with regard to the general fiber dynamics are currently ongoing.

292

293
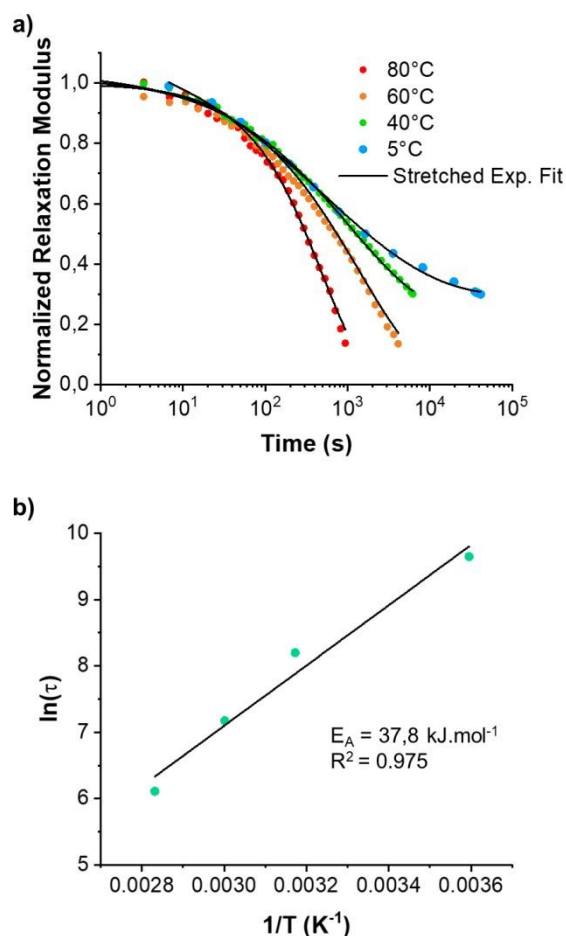
Fig. 9. Normalized stress relaxation modulus (shear mode) of BTP-C_{12} (a) at 5, 40, 60 and 80°C.
The data was measured consecutively on the same sample and normalized 20 seconds after strain
(1%) was applied. The characteristic relaxation times (in s) were plotted in a log plot (b) and fitted
using a linear fit to obtain the activation energy (E_A).

298 We finally aimed to assess the biocompatibility of the hydrogels. It is noteworthy to state that

299 instead of using hydrogel extracts, we designed an experimental system incubating L929 mouse

300 fibroblasts directly on a hydrogel layer, which allowed us to further investigate cell-to-hydrogel

301 interactions. Therefore, we tried to cover the bottom of wells in standard cell culture plates with

302 the hydrogel and subsequently seed cells onto the surface. However, following the same procedure

15

303   for preparing the hydrogels used for the rheological measurements, the BTP-C$_{12}$ system started to

304   gel at 20 to 30 v% water content which impeded a homogenous coverage of the culture plate surface

305   (Fig. S13). Therefore, we focused on the BTP-C$_6$ hydrogel with 2.5 wt% and 1 mol% of CL as the

306   exemplary system to evaluate cell interactions and biocompatibility. We added a predetermined

307   amount of BTP-C$_6$ hydrogel stock solution to a tissue culture (TC) treated 96-well culture plate

308   aiming at a final hydrogel thickness of 1.1 mm after evaporation of the solvent. The aimed thickness

309   ensured that the cells were only in contact with the hydrogel but not the bottom surface of the well.

310   Upon THF evaporation, we obtained intact BTP-C$_6$ hydrogels in the wells (Fig. S14). To ensure

311   full removal of the solvent and create conditions suitable for cell seeding, we washed the surface

312   of the hydrogels several times with PBS. Finally, we incubated the hydrogels treated with

313   Dulbecco's modified Eagle medium (D10) overnight at 37 °C under a humidified 5% (v/v) CO$_2$

314   atmosphere. It noteworthy that the thickness and consistency hydrogels did not change over the

315   course of this procedure despite being constantly covered by 100 μL of cell culture medium.

316   Following the preparation of the culture plate with hydrogel, L929 cells (50000 cells/mL per well)

317   were seeded in blank wells without hydrogel (control) and in wells covered with the hydrogels

318   (gel) in triplicate and the experiment was repeated for four different cell passages (P1, P2, P3, and

319   P4) (**Fig. 10**).
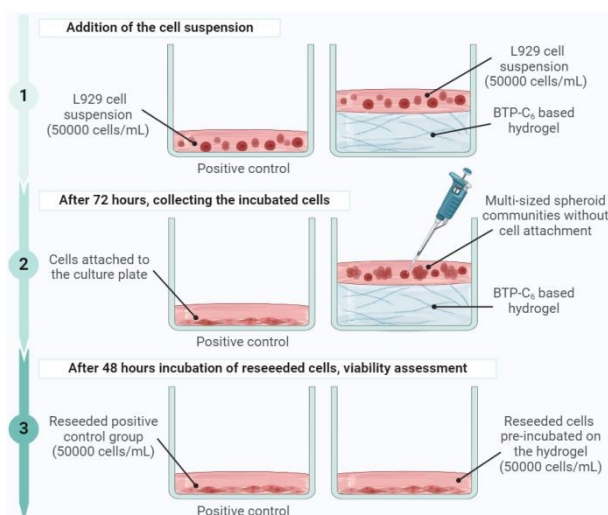
320

321   **Fig. 10.** Graphical representation of the experimental setup for the biocompatibility assessment of
322   BTP-C$_6$ hydrogel (Created with BioRender.com).

16

323   The cells were incubated for 72 hours, and afterwards they were imaged by light microscopy (**Fig.**

324   **11**). The cells did not attach to the surface of the hydrogel (**Fig. 11a**) but rather formed multi-sized

325   communities in spheroid shapes based on cell-to-cell aggregations. This is a quite common

326   behavior for the cells growing on the inert surfaces and indicates that the hydration shell around

327   the dense PEO chains on the fibers prevents protein adsorption and further cell interactions.[56-58]

328   After 72 hours of incubation, the cells were collected and reseeded in a TC treated 96-well culture

329   plate to understand whether the gels had any negative effect on the cell viability, morphology, and

330   attachment ability. Following 48 hours of incubation, the cells pre-incubated on the hydrogels were

331   able to re-attach to the culture plate. (**Fig. 11b**). In addition, there was no significant change in their

332   morphology compared to a control, so we can conclude that BTP-C_6 hydrogel had no detrimental

333   effect on L929 cells.

334
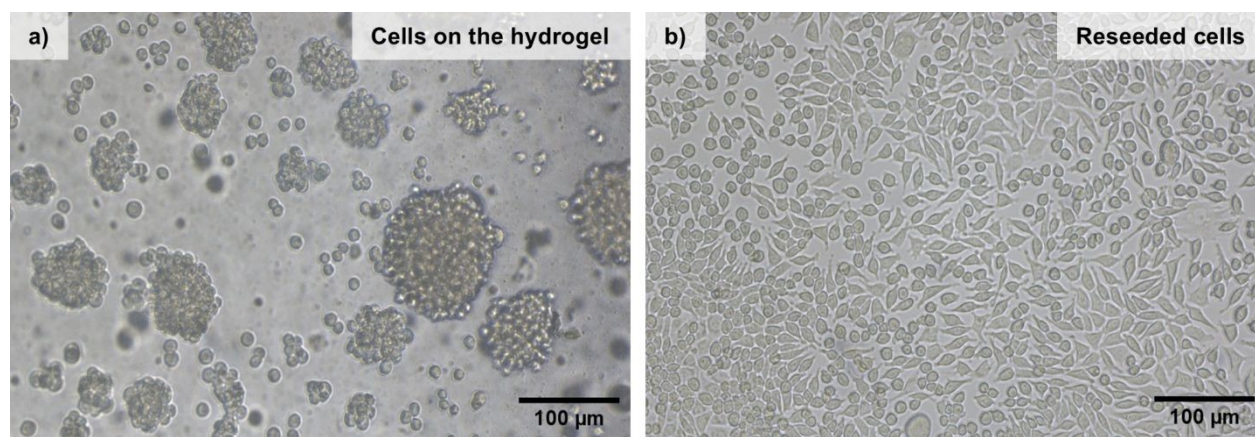
335   **Fig. 11.** Transmitted light microscopy images of L929 mouse fibroblast cells incubated on the
336   BTP-C_6 hydrogel for 72 hours (a; picture taken on the hydrogel) 48 hours of incubation for reseeded
337   cells collected from top of the hydrogel (b). Optical magnification is 10x and the scale bar is 100
338   μm.

339   The viability of the reseeded cells was quantitatively investigated *via* PrestoBlue™ assay. For all

340   passages, the mean relative metabolic activity values of the control groups were set as 100%. A

341   cell viability ≤ 70% is considered toxic according to DIN EN ISO 10993-5.[59] In comparison to the

342   control groups, the cells previously incubated on the hydrogels showed relative metabolic activities

343   in the range of 90% indicating that BTP-C_6 hydrogel had no toxic effect on L929 cells (**Fig. 12**).

344   Independent from the passage numbers, the mean relative metabolic activity was higher than 87%

345   for all gel groups in respect of the control groups and the mean values did not show any significant

17

346 variation from passage to passage (**Error! Reference source not found.**). In light of both
347 qualitative and quantitative observations, BTP-C$_6$ hydrogel can be considered biocompatible and
348 the formation of multi-sized spheroid on the hydrogel is currently under further investigation.
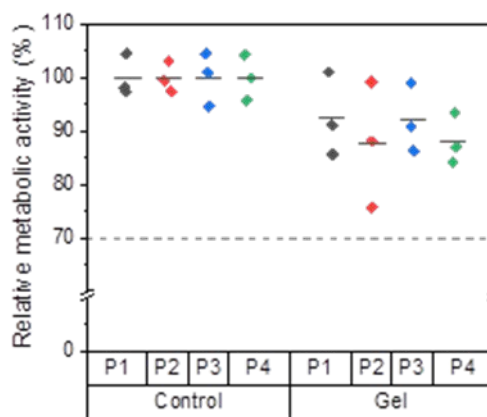
349

350 **Fig. 12.** Relative metabolic activity (%) of L929 mouse fibroblast cells growing on the BTP-C$_6$
351 hydrogel was determined by PrestoBlue™ assay. The experiments were conducted as triplicate for
352 four different passages represented as P1, P2, P3, and P4. Calculated mean values were depicted
353 as lines.

Conclusion

355 In conclusion we investigated the rheological properties of hydrogels formed from supramolecular
356 assembly of benzenetrispeptides with a C$_6$ and C$_{12}$ spacer and a conjugated PEO chain. The
357 introduction of a bifunctional crosslinker induced the hydrogel formation and we found that both
358 systems display fast recovery rates during step strain measurements. Varying the crosslinker
359 content had limited effect on the BTP-C$_{12}$ system, which was related to an inefficient integration
360 of the crosslinker. However, the BTP-C$_6$ system could be modified in terms of its shear modulus
361 over a range from 0.2 kPa up to nearly 2 kPa when increasing the crosslinker content from 0.1 to
362 10 mol%. Increasing the total concentration of the materials from 2.5 w% to 5 wt% caused another
363 significant increase of G' for BTP-C$_6$ system up to 8 kPa, while only a minor increase in G' (from
364 0.5 to 0.8 kPa) is observed for BTP-C$_{12}$, which is most likely again due to a limited integration of
365 the crosslinker. Temperature dependent measurements further revealed a thermo-stiffening
366 behavior of the BTP-C$_6$ system, which cannot be clarified at present, while the BTP-C$_{12}$ hydrogel

367 becomes weaker with the increasing temperature. Stress relaxation measurements of the latter

368 sample revealed an Arrhenius behavior indicating increasing dynamics at higher temperature.

369 Analyzing the shear dependent viscosity further revealed a strong shear-thinning effect of all tested

370 samples, which facilitates effortless injections even through thinnest needles. A fluorescein

371 containing BTP-C_6 hydrogel could therefore be easily injected into a chicken breast as muscle

372 tissue sample applying only a minor force. The hydrogel distributes between muscle cords but,

373 more importantly, is able to reform even within this tissue and remains at the injection side even

374 after massaging the muscle. Direct incubation of L929 mouse fibroblast cells on the hydrogel

375 confirmed that the dense PEO-shell on the fibers prevents an attachment of the cells and spheroid

376 like communities are formed. Nevertheless, reseeding of these cells and comparison to a control

377 resulted in a relative metabolic activity over 87% independent from the passage number, and no

378 signs of changes in cell morphology or behavior were observed. Overall, these experiments prove

379 a high biocompatibility of these injectable supramolecular hydrogels and the tunable shear modulus

380 of the BTP-C_6 system allows adaption of the hydrogel to the specific strength of different soft

381 tissues such as brain, pancreas, or lung resembling it an attractive material for application as drug

382 depot or in tissue engineering.[60-63]

383

Methods and Materials

385 All reagents and solvents were commercial products purchased from Merck, ABCR, Iris BioTech,
386 Rapp Polymere or TCI and were used without further purification. The BTP building blocks were
387 prepared according to procedures described in literature.[28, 35] Details on the synthesis of the
388 crosslinker are provided in the supplementary information.

Gel preparation

390 The hydrogels preparation procedure is based on the solvent switch and gel preparation method
391 described in the following.[28, 36] The gels were prepared by weighing in the lyophilized building
392 blocks and crosslinker in a 20 mL vial with wide neck. 0.75 mL THF were added, the vial was
393 closed, and the solids were dissolved using sonication and light heating. Afterwards the samples
394 were mixed using a magnetic stirrer for 30 min. to the closed vial 1.5 mL of water were added at a
395 speed of 1 mL h^{-1} using a syringe pump. Lastly the cap was removed to slowly evaporate the THF
396 until the weight of the gel was 1.5 g. Lastly the gel was transferred to the rheometer.

Rheology measurements

398 The oscillatory dynamic measurements were performed with a Physica Modular Compact
399 MCR102 Rheometer from Anton Paar (Germany). Mechanical properties of the viscoelastic
400 hydrogel material were assayed using a parallel (PP 25 sandblasted)-plate geometry. The linear
401 viscoelastic regime of the samples was obtained from amplitude sweep experiments that were
402 performed from 0.1 to 200% strain at 6.36 rad s^{-1} angular frequency. Frequency sweep
403 measurements were recorded from 0.1 to 100 rad s^{-1} at 1% strain. Measurements were performed
404 at 20 °C unless stated otherwise. For measurements above 20 °C paraffin oil was added around the
405 sample and geometries to hinder the sample drying out due to water evaporation.

Biological investigation

407 L929 cells (CLS Cell Lines Service GmbH, Eppelheim, Germany) were cultured in TC treated cell
408 culture flasks (Greiner Bio-One International GmbH and Labsolute Th. Geyer GmbH & Co. KG)
409 in the presence of Dulbecco's modified Eagle medium (D10) (2 mM l-glutamine (Biochrom,
410 Germany) supplemented with 10% fetal calf serum (FCS, Capricorn Scientific, Germany), 100 U

411   mL^{-1} penicillin, and 100 μg mL^{-1} streptomycin (Biochrom)) at 37 °C under a humidified 5% (v/v)

412   CO_2 atmosphere. Dulbecco's phosphate-buffered saline (1x) (DPBS) and trypsin-EDTA

413   (Capricorn Scientific GmbH, Germany) were used for each cell passaging. The cells with the

414   passage numbers 22 (P1), 23 (P2), 24 (P3), and 25 (P5) showing ≥97% viability were used.

415   For the cell viability assessment, hydrogel stock solution was prepared strictly following the above-

416   mentioned preparation methodology. Under sterile environment, predetermined amount of

417   hydrogel stock solution (57 μL) was added to each well of TC treated 96-well cell culture plates

418   (VWR International GmbH) by aiming 1 to 1.2 mm gel thickness (Fig. S16). After evaporation of

419   THF from the system in a sterile environment, hydrogels formed and a serial of washing with PBS

420   was conducted to adjust pH of the system. Afterwards, 100 μL of DMEM was added in each well

421   containing hydrogel. The plate was incubated overnight at 37 °C under a humidified 5% (v/v) CO_2

422   atmosphere for the next day's cell seeding. The following day, L929 cells were seeded (5000 cells

423   per well) both in the wells without gels (positive control) and with the gels in triplicate. The cells

424   were incubated for three days at 37 °C under a humidified 5% (v/v) CO_2 atmosphere.

425   After 72 hours, control groups were collected by trypsinization. However, the cells growing on the

426   gels were directly collected since the cells did not attach to the surface of the hydrogel. For each

427   sample, the viability and number of the cells were determined by a cell counter (fluidlab R-300

428   anvajo GmbH, Dresden, Germany). 5000 cells from each sample were reseeded in a TC treated 96-

429   well cell culture plate and the cells were incubated for two days at 37 °C under a humidified 5%

430   (v/v) CO_2 atmosphere. After 48 hours, the viability assessment was conducted.

431   Relative metabolic activity of viable L929 mouse fibroblast cells were determined by PrestoBlue™

432   assay (Thermo Fisher Scientific) following DIN EN ISO 10993-5. 10% (v/v) PrestoBlue™

433   solution, which was prepared according to the manufacturer's instructions, was added to each well.

434   Afterwards, the cells were further incubated at 37 °C for 45 min and finally the fluorescence was

435   measured with a multi-plate reader (Infinite M200 PRO Microplate Reader, Tecan, Switzerland)

436   at λ_{Ex} = 560 nm/ λ_{Em} = 590 nm. The relative viability (%) of the cells was calculated as in equation

437   3:

438   $$Relative\ viability\ (\%) = \frac{FI_{sample}-FI_0}{FI_{Ctrl}-FI_0} \times 100, \textbf{(3)}$$

21

439   where FI_{Sample}, FI_0, and FI_{Ctrl} represent the fluorescence intensity of cell growing on the hydrogel,

440   negative control (cell culture medium without cells), and control cells growing in the native

441   condition (100 % viability), respectively.

442   In addition to the viability assessment, cells were observed with a transmitted light microscope

443   (Axio Oberserver Vert.A1, Zeiss, Germany) with a 10× objective using brightfield imaging.

444   Images were recorded by ZEN lite software (2012, Zeiss).

445   For the statistical analysis, OriginPro2022b software was used. The mean relative metabolic

446   activity of each group was calculated as mean ± SD. In addition, a one-way analysis of variance

447   (ANOVA) was conducted. At level 0.05, there was no significant difference among mean relative

448   metabolic activity of the passages.

Conflict of interests

450   There are no conflicts to declare.

Acknowledgments

References

460   1.   R. Dong, Y. Pang, Y. Su and X. Zhu, *Biomater. Sci.*, 2015, **3**, 937-954.

461   2.   X. Du, J. Zhou, J. Shi and B. Xu, *Chem. Rev.*, 2015, **115**, 13165-13307.

462   3.   J. Y. C. Lim, Q. Lin, K. Xue and X. J. Loh, *Materials Today Advances*, 2019, **3**, 100021.

463   4.   S. Khan, A. Ullah, K. Ullah and N.-u. Rehman, *Designed Monomers and Polymers*, 2016, **19**, 456-
464   478.

465   5.   M. Santin, S. J. Huang, S. Iannace, L. Ambrosio, L. Nicolais and G. Peluso, *Biomaterials*, 1996,
466   **17**, 1459-1467.

22

Journal of Materials Chemistry B Accepted Manuscript

467　6.　K. Kowalczuk, P. Mons, H. Ulrich, V. Wegner, J. Brendel, A. Mosig and F. Schacher, *Macromol.*
468　　　*Biosci.*, 2023, DOI: 10.1002/mabi.202300230.
469　7.　R. Yoshida, K. Uchida, Y. Kaneko, K. Sakai, A. Kikuchi, Y. Sakurai and T. Okano, *Nature*, 1995,
470　　　**374**, 240-242.
471　8.　L. A. Estroff and A. D. Hamilton, *Chem. Rev.*, 2004, **104**, 1201-1218.
472　9.　J. Raeburn, A. Zamith Cardoso and D. J. Adams, *Chem. Soc. Rev.*, 2013, **42**, 5143-5156.
473　10.　X. Wang and C. Feng, *WIREs Nanomedicine and Nanobiotechnology*, 2023, **15**, e1847.
474　11.　R. F. Q. Grenfell, L. M. Shollenberger, E. F. Samli and D. A. Harn, *Clin. Vaccine Immunol.*, 2015,
475　　　**22**, 336-343.
476　12.　Y. Tian, H. Wang, Y. Liu, L. Mao, W. Chen, Z. Zhu, W. Liu, W. Zheng, Y. Zhao, D. Kong, Z.
477　　　Yang, W. Zhang, Y. Shao and X. Jiang, *Nano Lett.*, 2014, **14**, 1439-1445.
478　13.　M. Guvendiren, H. D. Lu and J. A. Burdick, *Soft Matter*, 2012, **8**, 260-272.
479　14.　Q. Wang, J. Wang, Q. Lu, M. S. Detamore and C. Berkland, *Biomaterials*, 2010, **31**, 4980-4986.
480　15.　M. Guo, L. M. Pitet, H. M. Wyss, M. Vos, P. Y. Dankers and E. W. Meijer, *J. Am. Chem. Soc.*,
481　　　2014, **136**, 6969-6977.
482　16.　M. M. C. Bastings, S. Koudstaal, R. E. Kieltyka, Y. Nakano, A. C. H. Pape, D. A. M. Feyen, F. J.
483　　　van Slochteren, P. A. Doevendans, J. P. G. Sluijter, E. W. Meijer, S. A. J. Chamuleau and P. Y. W.
484　　　Dankers, *Adv. Healthc. Mater.*, 2014, **3**, 70-78.
485　17.　P. Y. W. Dankers, M. J. A. van Luyn, A. Huizinga-van der Vlag, G. M. L. van Gemert, A. H.
486　　　Petersen, E. W. Meijer, H. M. Janssen, A. W. Bosman and E. R. Popa, *Biomaterials*, 2012, **33**,
487　　　5144-5155.
488　18.　E. K. Johnson, D. J. Adams and P. J. Cameron, *J. Mater. Chem.*, 2011, **21**, 2024-2027.
489　19.　C. Yan, A. Altunbas, T. Yucel, R. P. Nagarkar, J. P. Schneider and D. J. Pochan, *Soft Matter*, 2010,
490　　　**6**, 5143-5156.
491　20.　J. J. Van Gorp, J. A. Vekemans and E. W. Meijer, *J. Am. Chem. Soc.*, 2002, **124**, 14759-14769.
492　21.　M. de Loos, J. H. van Esch, R. M. Kellogg and B. L. Feringa, *Tetrahedron*, 2007, **63**, 7285-7301.
493　22.　C. M. A. Leenders, T. Mes, M. B. Baker, M. M. E. Koenigs, P. Besenius, A. R. A. Palmans and E.
494　　　W. Meijer, *Mater. Horiz.*, 2014, **1**, 116-120.
495　23.　S. Bernhard and M. W. Tibbitt, *Adv. Drug Delivery Rev.*, 2021, **171**, 240-256.
496　24.　G. Zhang, Y. Chen, Y. Deng, T. Ngai and C. Wang, *ACS Macro Lett.*, 2017, **6**, 641-646.
497　25.　J. Li, X. Li, X. Ni, X. Wang, H. Li and K. W. Leong, *Biomaterials*, 2006, **27**, 4132-4140.
498　26.　L. Li, B. Yan, J. Yang, L. Chen and H. Zeng, *Adv. Mater.*, 2015, **27**, 1294-1299.
499　27.　P. Y. W. Dankers, T. M. Hermans, T. W. Baughman, Y. Kamikawa, R. E. Kieltyka, M. M. C.
500　　　Bastings, H. M. Janssen, N. A. J. M. Sommerdijk, A. Larsen, M. J. A. van Luyn, A. W. Bosman, E.
501　　　R. Popa, G. Fytas and E. W. Meijer, *Adv. Mater.*, 2012, **24**, 2703-2709.
502　28.　F. V. Gruschwitz, F. Hausig, P. Schüler, J. Kimmig, S. Hoeppener, D. Pretzel, U. S. Schubert, S.
503　　　Catrouillet and J. C. Brendel, *Chem. Mater.*, 2022, **34**, 2206-2217.
504　29.　J.-L. Li and X.-Y. Liu, *Adv. Funct. Mater.*, 2010, **20**, 3196-3216.
505　30.　S. Correa, A. K. Grosskopf, H. Lopez Hernandez, D. Chan, A. C. Yu, L. M. Stapleton and E. A.
506　　　Appel, *Chem. Rev.*, 2021, **121**, 11385-11457.
507　31.　D. L. Taylor and M. in het Panhuis, *Adv. Mater.*, 2016, **28**, 9060-9093.
508　32.　A. P. Nowak, V. Breedveld, L. Pakstis, B. Ozbas, D. J. Pine, D. Pochan and T. J. Deming, *Nature*,
509　　　2002, **417**, 424-428.
510　33.　L. A. Haines-Butterick, D. A. Salick, D. J. Pochan and J. P. Schneider, *Biomaterials*, 2008, **29**,
511　　　4164-4169.
512　34.　F. V. Gruschwitz, M.-C. Fu, T. Klein, R. Takahashi, T. Higashihara, S. Hoeppener, I. Nischang, K.
513　　　Sakurai and J. C. Brendel, *Macromolecules*, 2020, **53**, 7552-7560.
514　35.　T. Klein, H. F. Ulrich, F. V. Gruschwitz, M. T. Kuchenbrod, R. Takahashi, S. Fujii, S. Hoeppener,
515　　　I. Nischang, K. Sakurai and J. C. Brendel, *Polym. Chem.*, 2020, **11**, 6763-6771.

Journal of Materials Chemistry B Accepted Manuscript

516   36.   F. V. Gruschwitz, T. Klein, M. T. Kuchenbrod, N. Moriyama, S. Fujii, I. Nischang, S. Hoeppener,
517   K. Sakurai, U. S. Schubert and J. C. Brendel, *ACS Macro Lett.*, 2021, **10**, 837-843.
518   37.   T. Klein, H. F. Ulrich, F. V. Gruschwitz, M. T. Kuchenbrod, R. Takahashi, S. Hoeppener, I.
519   Nischang, K. Sakurai and J. C. Brendel, *Macromol. Rapid Commun.*, 2021, **42**, e2000585.
520   38.   H. F. Ulrich, F. V. Gruschwitz, T. Klein, N. Ziegenbalg, D. T. N. Anh, S. Fujii, S. Hoeppener, K.
521   Sakurai and J. C. C. Brendel, *Chem. Eur. J.*, 2024, **30**, e202400160.
522   39.   P. Bertsch, M. Diba, D. J. Mooney and S. C. G. Leeuwenburgh, *Chem. Rev.*, 2023, **123**, 834-873.
523   40.   M. H. Chen, L. L. Wang, J. J. Chung, Y.-H. Kim, P. Atluri and J. A. Burdick, *ACS Biomaterials*
524   *Science & Engineering*, 2017, **3**, 3146-3160.
525   41.   R. S. H. Wong, M. Ashton and K. Dodou, *Pharmaceutics*, 2015, **7**, 305-319.
526   42.   N. Paxton, W. Smolan, T. Böck, F. Melchels, J. Groll and T. Jungst, *Biofabrication*, 2017, **9**,
527   044107.
528   43.   J. S. Weston, J. H. Harwell and B. P. Grady, *Soft Matter*, 2017, **13**, 6743-6755.
529   44.   J. C. P. Hollister, A. C. Wang, W. Kim, C. C. Giza, M. L. Prins and H. P. Kavehpour, *Frontiers in*
530   *Physics*, 2023, **11**.
531   45.   https://www.immunize.org/wp-content/uploads/catg.d/p2020a.pdf, (accessed 11.08.2024).
532   46.   R. P. Watt, H. Khatri and A. R. G. Dibble, *Int. J. Pharm.*, 2019, **554**, 376-386.
533   47.   L. Wu, H. Li, Y. Wang, C. Liu, Z. Zhao, G. Zhuang, Q. Chen, W. Zhou and J. Guo, *Eur. J. Pharm.*
534   *Biopharm.*, 2024, **197**, 114221.
535   48.   J. Cheng, D. Amin, J. Latona, E. Heber-Katz and P. B. Messersmith, *ACS Nano*, 2019, **13**, 5493-
536   5501.
537   49.   R. E. Kieltyka, A. C. H. Pape, L. Albertazzi, Y. Nakano, M. M. C. Bastings, I. K. Voets, P. Y. W.
538   Dankers and E. W. Meijer, *J. Am. Chem. Soc.*, 2013, **135**, 11159-11164.
539   50.   S. Xian and M. J. Webber, *J. Mater. Chem. B*, 2020, **8**, 9197-9211.
540   51.   G. Chaudhary, A. Ghosh, N. A. Bharadwaj, J. G. Kang, P. V. Braun, K. S. Schweizer and R. H.
541   Ewoldt, *Macromolecules*, 2019, **52**, 3029-3041.
542   52.   P. de Almeida, M. Jaspers, S. Vaessen, O. Tagit, G. Portale, A. E. Rowan and P. H. J. Kouwer, *Nat*
543   *Commun*, 2019, **10**, 609.
544   53.   R. D. Chakravarthy, I. Sahroni, C. W. Wang, M. Mohammed and H. C. Lin, *ACS Nano*, 2023, **17**,
545   11805-11816.
546   54.   W. Denissen, J. M. Winne and F. E. Du Prez, *Chem. Sci.*, 2016, **7**, 30-38.
547   55.   R. G. Ricarte and S. Shanbhag, *Polym. Chem.*, 2024, **15**, 815-846.
548   56.   L. Chen, C. Yan and Z. Zheng, *Mater. Today*, 2018, **21**, 38-59.
549   57.   B. D. Ippel, H. M. Keizer and P. Y. W. Dankers, *Adv. Funct. Mater.*, 2019, **29**, 1805375.
550   58.   H. Shen, S. Cai, C. Wu, W. Yang, H. Yu and L. Liu, *Micromachines*, 2021, **12**, 96.
551   59.   *DIN EN ISO 10993-5:2009-10, Biological evaluation of medical devices-Part5: Test for in vitro*
552   *cytotoxicity*, European Standard EN ISO 10993-5, Brussels.
553   60.   D. M. Tremmel, S. D. Sackett, A. K. Feeney, S. A. Mitchell, M. D. Schaid, E. Polyak, P. J.
554   Chlebeck, S. Gupta, M. E. Kimple, L. A. Fernandez and J. S. Odorico, *Scientific Reports*, 2022, **12**,
555   7188.
556   61.   G. Burgstaller, B. Oehrle, M. Gerckens, E. S. White, H. B. Schiller and O. Eickelberg, *European*
557   *Respiratory Journal*, 2017, **50**, 1601805.
558   62.   L. Glorieux, L. Vandooren, S. Derclaye, S. Pyr dit Ruys, P. Oncina-Gil, A. Salowka, G. Herinckx,
559   E. Aajja, P. Lemoine, C. Spourquet, H. Lefort, P. Henriet, D. Tyteca, F. M. Spagnoli, D. Alsteens,
560   D. Vertommen and C. E. Pierreux, *International Journal of Molecular Sciences*, 2023, **24**, 10268.
561   63.   S. Budday, T. C. Ovaert, G. A. Holzapfel, P. Steinmann and E. Kuhl, *Archives of Computational*
562   *Methods in Engineering*, 2020, **27**, 1187-1230.

563

1 **Injectable biocompatible hydrogels with tunable strength based on**

2 **crosslinked supramolecular polymer nanofibers**

3 Hans F. Ulrich,[a,b] Ceren C. Pihlamägi,[a,b] Tobias Klein,[a,b] Camille Bakkali-Hassani,[c] Sylvain

4 Catrouillet,[c] Johannes C. Brendel,[a,b,d,e],*

5 a   Laboratory of Organic and Macromolecular Chemistry (IOMC), Friedrich Schiller University

6   Jena, Humboldtstr. 10, 07743 Jena, Germany

7 b   Jena Center for Soft Matter (JCSM), Friedrich Schiller University Jena, Philosophenweg 7,

8   07743 Jena, Germany

9 c   ICGM, Univ. Montpellier, CNRS, ENSCM, 34095 Montpellier, France

10 d   Macromolecular Chemistry I, University of Bayreuth, Universitätsstr. 30, 95447 Bayreuth,

11   Germany

12 e   Institute of Macromolecular Research (BIMF) and Bavarian Polymer Institute (BPI),

13   University of Bayreuth, Universitätsstr. 30, 95447 Bayreuth, Germany

14 *corresponding author: johannes.brendel@uni-jena.de

15 Keywords: Supramolecular polymer bottlebrushes, polymer networks, self-assembly, shear-
16 thinning, stealth properties.

Data availability statement

18 The data supporting this article have been included as part of the Supplementary Information

1